Contact mechanics between the human finger and a touchscreen under electroadhesion

Mehmet Ayyildiz[a,b,c], Michele Scaraggi[a,d], Omer Sirin[c], Cagatay Basdogan[c], and Bo N. J. Persson[a,e,1]

[a]Theory 1, Peter Grünberg Institute-1, Forschungszentrum Jülich, 52425 Jülich, Germany; [b]Faculty of Engineering and Natural Sciences, Istanbul Bilgi University, 34060 Istanbul, Turkey; [c]College of Engineering, Koc University, 34450 Istanbul, Turkey; [d]Dipartimento di Ingegneria dell'Innovazione, Università del Salento, 73100 Lecce, Italy; and [e]Multiscale Consulting, 52425 Jülich, Germany

Edited by Erio Tosatti, International School for Advanced Studies, Trieste, Italy, and approved October 29, 2018 (received for review July 9, 2018)

The understanding and control of human skin contact against technological substrates is the key aspect behind the design of several electromechanical devices. Among these, surface haptic displays that modulate the friction between the human finger and touch surface are emerging as user interfaces. One such modulation can be achieved by applying an alternating voltage to the conducting layer of a capacitive touchscreen to control electroadhesion between its surface and the finger pad. However, the nature of the contact interactions between the fingertip and the touchscreen under electroadhesion and the effects of confined material properties, such as layering and inelastic deformation of the stratum corneum, on the friction force are not completely understood yet. Here, we use a mean field theory based on multiscale contact mechanics to investigate the effect of electroadhesion on sliding friction and the dependency of the finger–touchscreen interaction on the applied voltage and other physical parameters. We present experimental results on how the friction between a finger and a touchscreen depends on the electrostatic attraction between them. The proposed model is successfully validated against full-scale (but computationally demanding) contact mechanics simulations and the experimental data. Our study shows that electroadhesion causes an increase in the real contact area at the microscopic level, leading to an increase in the electrovibrating tangential frictional force. We find that it should be possible to further augment the friction force, and thus the human tactile sensing, by using a thinner insulating film on the touchscreen than used in current devices.

electroadhesion | haptics | touchscreens | skin friction | multiscale contact mechanics

Sliding friction depends sensitively on the nature of the materials involved, in particular at the sliding interface where the surface topography, contamination films, and the atomic and molecular nature of the contacting surfaces strongly influence the friction. However, the sliding friction also depends on external conditions such as temperature and the humidity and on mechanical vibrations and electric fields. For example, it has been shown that ultrasonic vibrations act to reduce friction—for example, between the finger and a counter surface (1). Similarly, an applied electric potential between two solids often results in the accumulation of charges of opposite sign on the contacting surfaces. This results in an electrostatic attraction, denoted "electroadhesion," which adds to the external load (squeezing-force) and increases the sliding friction force.

The electrical attraction between a charged surface and human skin was discovered by Johnsen and Rahbek (2) in 1923. Later, in 1953, Mallinckrodt (3) reported an increase in the friction during touch when an alternating voltage is applied to an insulated aluminum plate. This effect is now intensively studied for grippers in the areas of industrial and surgical robotics (4–6) and also in the context of touchscreen applications where one is interested in modulating the friction between the human finger and the touchscreen to display haptic feedback to the user for augmented or alternative sensorial experience (7, 8). Hence, understanding the physics behind this bioelectromechanical interaction can provide the step forward into the development of this technology not only for online shopping, education, gaming, and data visualization but also for rehabilitative medicine and user interface development for blind people.

Nowadays, electric capacitive displays have become one of the most essential parts of smartphones, tablets, and notebooks. These screens detect the finger position and help the user interact with text, pictures, and other digital information. One important effort to make this interaction more effective is to display tactile feedback to the user through the use of electrostatic forces to increase the physicality of touch interaction and/or to improve haptic perception (9–14). When an alternating electric potential is applied to the conductive layer of a surface capacitive touchscreen, the insulating layer on the glass plate and the finger are polarized by induction. Thus, an electrostatic attraction force is generated between the finger and the counter surface, which increases the sliding friction between them. This phenomenon was referred to as "electrovibration" by Grimnes (15), who also reported that the perceived tactile sensation depends on the roughness and moisture of the finger.

In Fig. 1, we schematically show the physical processes and related length scales leading to tactile sensing in the contact between finger and electrostatically actuated touchscreen. The skin shows graded mechanobiological properties with specific nerve receptors placed at specific depths from the outermost surface (Fig. 1*B*). The latter is characterized by the stratum corneum

Significance

The technology for generating tactile feedback on a touchscreen via electroadhesion is already available—and straightforward to implement—but the knowledge on human skin contact mechanics is limited. To better understand the contact mechanism between the finger pad and touchscreen under electroadhesion, we investigated the sliding friction as a function of normal force and voltage using (*i*) a mean field theory based on multiscale contact mechanics, (*ii*) a full-scale computational contact mechanics study, and (*iii*) experiments performed on a custom-made tribometer. We show that the real contact area and the electroadhesion force depend strongly on the skin surface roughness and on the nature of the touchscreen coating. Thus, by reducing the effective thickness of the latter, the human tactile sensing can be drastically enhanced.

Author contributions: M.A., M.S., O.S., C.B., and B.N.J.P. designed research, performed research, analyzed data, and wrote the paper.

The authors declare no conflict of interest.

This article is a PNAS Direct Submission.

Published under the PNAS license.

[1]To whom correspondence should be addressed. Email: B.Persson@fz-juelich.de.

This article contains supporting information online at www.pnas.org/lookup/suppl/doi:10.1073/pnas.1811750115/-/DCSupplemental.

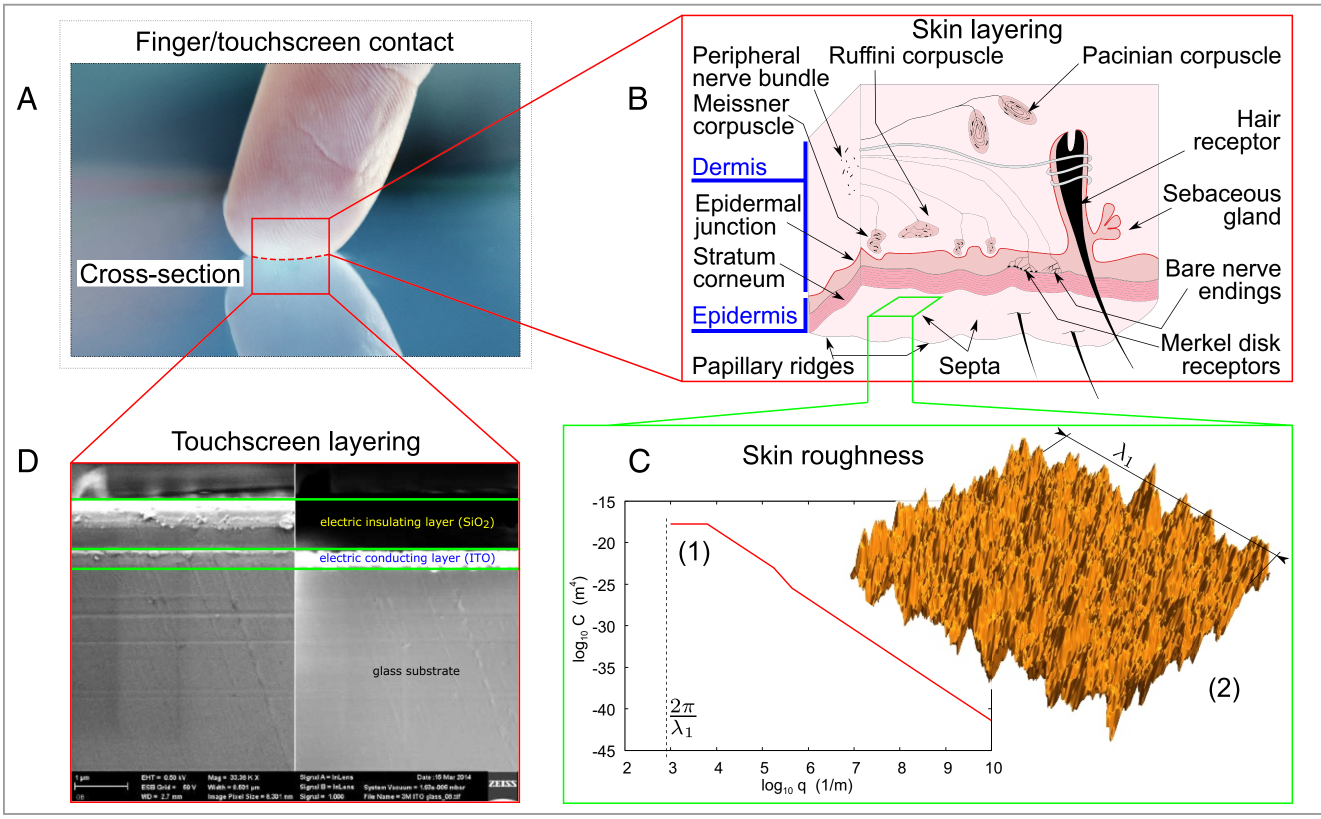

Fig. 1. (*A*) Physical processes and related length scales leading to tactile sensing during contact between finger and touchscreen under electroadhesion. (*B*) Schematic of the layered structure of the generic human skin with indication of the relevant biological clues and nerve receptors. (*C*) The surface roughness PSD as a function of the wavenumber (log–log scale) calculated from the skin surface topography reported in refs. 16 and 17. The PSD has the rms roughness amplitude 22 μm and the rms slope 0.91. The linear region for $q > 4 \times 10^5$ m^{-1} corresponds to a Hurst exponent $H = 0.86$. The 3D surface roughness corresponds to a realization of the PSD. (*D*, *Left*) Cross-section image of a capacitive touchscreen (model SCT-3250, 3M) obtained by field emission scanning electron microscopy (FESEM, Zeiss Ultra Plus). (*Right*) The same image is reported with an improved contrast to highlight the different layers of the cross-section: an electric insulator layer (SiO_2) with a thickness of ≈ 1 μm, an electric conducting layer (ITO) with a thickness of ≈ 250 nm, and glass substrate.

(SC), which consists of corneocytes (dead cells) with high keratin content embedded in a lipid medium. The SC is characterized by a peculiar papillary ridge patterning and at shorter length scales (higher magnification) by a random surface roughness (16, 17), whose spectral characteristics and 3D roughness map [corresponding to a realization of the power spectral density (PSD)] are shown in Fig. 1*C*. The touchscreen cross-section is also a layered structure with an electric insulator layer (SiO_2) on top of an electric conducting layer (ITO), the latter bonded onto a glass substrate (Fig. 1*D*).

In this paper, we present a theoretical model, supported by experiments, for the prediction of the friction force resulting from the electrostatic attraction between finger and touchscreen. The dependency of the finger/touchscreen interaction on the applied voltage, as well as on the applied finger load, is modeled using a mean field contact mechanics theory, whose stochastic formulation is validated against the results of Boundary Element Method (BEM, summarized in *SI Appendix*) simulations. The predictions made by the theory are then compared with the experimental data collected by a custom-made tribometer, able to acquire both the normal and tangential finger–touchscreen interaction forces during sliding. In the experiments, the electroadhesion forces are modulated by changing the magnitude of alternating voltage applied to the touchscreen. Finally, a discussion on the origin and enhancement of the friction due to electroadhesion is provided, along with the corresponding design criteria.

Results

Mean Field Contact Mechanics. The skin–touchscreen interaction has a multiscale nature, as schematically described in Fig. 1. In particular, the electromechanical layering properties of the interface have been approximated with the schema reported in Fig. 2 *A*, *1*. In general, the SC behaves as a nonlinear viscoelastic solid. In the dry state, it deforms in a nearly irreversible manner when the contact pressure becomes high enough. Thus, it can be approximated by an elastoplastic model with the Youngs modulus $E \approx 1$ GPa and the penetration harness $\sigma_Y \approx 50$ MPa. In the wet state, the elastic modulus is very low (of order 10 MPa), resulting in much smaller contact pressures, and the SC can be described as an elastic (or viscoelastic) solid.

Consider two conducting solids with insulating surface layers of thickness d_1 and d_2 (respectively, for the touchscreen insulating layer and SC) and relative dielectric constants ϵ_1 and ϵ_2. Both solids have nominally flat surfaces, but one surface (namely that of the SC) has multiscale surface roughness. We define the effective thickness of the insulating layer as $h_0 = d_1/\epsilon_1 + d_2/\epsilon_2$. An electric voltage difference V exists between the two conducting solids, which make random atomic contacts over a fraction A/A_0 of the nominal contact area A_0 (in the schematic $A = 0$). Thus, the interface separation distance $u = u(x,y)$, which depends on the lateral coordinate (x,y), is a random process.

The contact area measured at macroscale (nominal contact area) is not a good estimation of the true contact interface

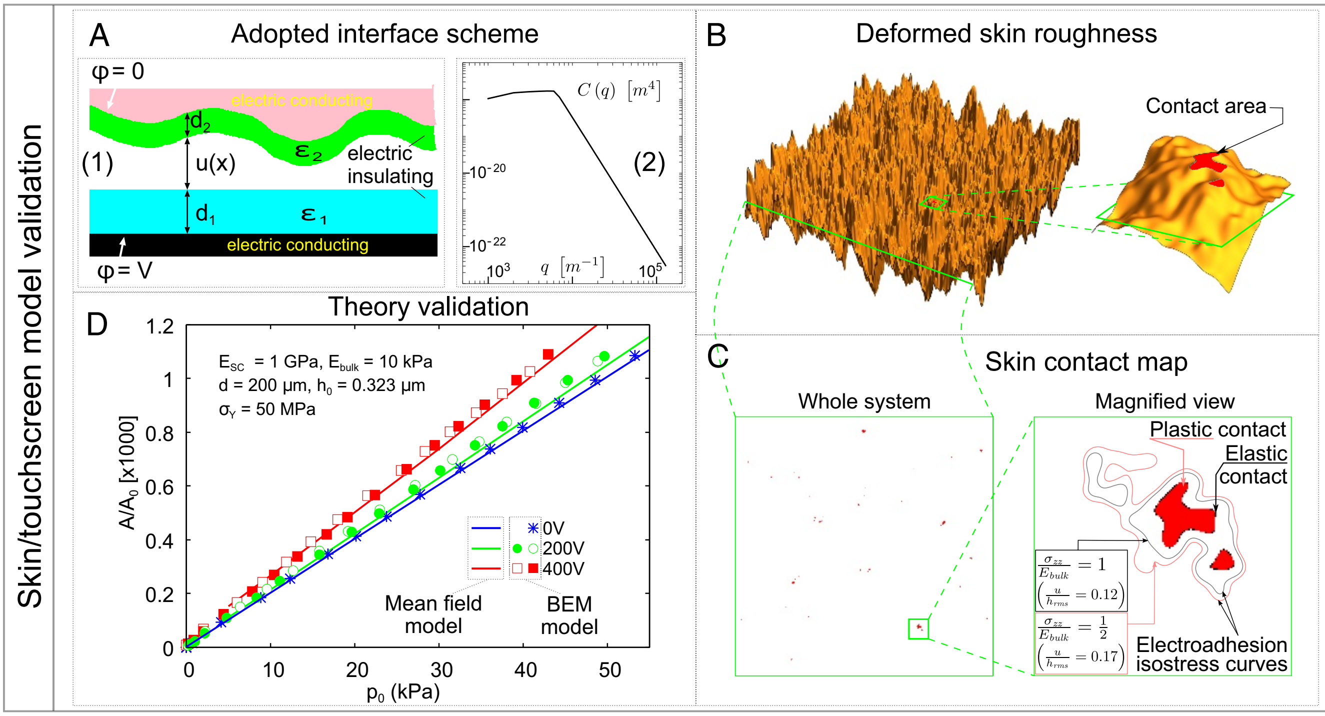

Fig. 2. Skin–touchscreen mean field model properties and validation against the predictions of BEM simulations. (*A*) Adopted microcontact model: an elastic solid with surface roughness above a rigid solid with a flat surface (*1*) and the PSD used for the comparison of the models (*2*). An electric voltage difference *V* occurs between the two conducting solids. (*B*) BEM-predicted roughness upon contact, with a magnified view of the surface and representation of the contact domain. The rough contact is simulated with 16 divisions at the small roughness wavelength. (*C*) BEM-predicted skin microcontact map, with magnified view of the map and indication of the contact domain. The black and red contour lines show the electroadhesive iso-stress curves around the true contact areas (h_{rms} is the rms surface roughness). (*D*) Comparison between the normalized contact area as a function of the contact pressure, at different values of applied voltage difference across the interface.

between fingertip and a smooth countersurface (18). Hence, a multiscale contact mechanics theory considering the finger surface properties at different length scales must be implemented to better understand the mechanics of the electroadhesion phenomenon. In this study, a mean field theory taking into account the surface roughness, surface plasticity, and finger layering (see *Materials and Methods*) is validated against deterministic contact electromechanics simulations for dry skin performed by BEM (19). Fig. 2 *A*, *2* shows the roughness PSD used in the comparison, whereas the remaining electromechanics parameters are reported in Fig. 2*D*. The contact setup is the same as in Fig. 2 *A*, *1*. Fig. 2*B* shows, for one roughness realization, the BEM-predicted finger roughness upon reaching a normalized contact area of $A/A_0 \approx 10^{-3}$, with a magnified view of the surface (and its contact spot). In Fig. 2*C*, we report the BEM-predicted skin microcontact map (white is for noncontact), with a magnified view of the map. In the magnification, the black and red contour lines show the complex patterns produced by the electroadhesive iso-stress curves around the true contact areas, revealing that an important contribution to electroadhesion, which is more effective in the contact domains (where interface separation is zero), is definitely provided by noncontact areas as well. Finally, in Fig. 2*D*, we report the normalized contact area A/A_0 as a function of the contact pressure p_0 for different values of applied voltage difference across the interface. The markers are the outputs of the BEM simulations for two realizations of the PSD given in Fig. 2 *A*, *2*, whereas the solid lines are the outputs of the mean field theory. The comparison has been limited to a range of normalized contact areas that is of interest for the application. We observe a very good agreement between the results of the stochastic and deterministic contact models.

Comparison with Experiments. In Fig. 3*A*, we show the schematic of the experimental setup. We found that the apparent contact area A_0 depends weakly on the normal force, where in our experiments the nominal contact pressure $p_0 = F_N/A_0$ varies between 3 kPa and 20 kPa. We report the typical friction force measured in our setup as a function of time in Fig. 3*B*. The green line is obtained by an oscillating electric potential $\phi = V_0 \cos(\omega_0 t)$ [with $V_0 = 200$ V and $f_0 = \omega_0/(2\pi) = 125$ Hz] applied to the touchscreen. The blue line is for the case without the applied electric potential. The normal force applied by the finger is $F_N = 1$ N in both cases. We note that (in the green curve) the main frequency of the friction signal is 250 Hz, exactly twice the frequency of the applied electric potential, as expected from the theory (see Eq. **1**). In Fig. 3*C*, we compare the friction coefficient estimated from the experimental data (markers) with the one predicted by theory (solid lines). The kink in the calculated black curve ($V_0 = 200$ V curve) is due to the approximate way we include finite-size effects. In the calculation, we used the SC Young's modulus $E = 40$ MPa, corresponding to semiwet skin. The frictional shear stress τ_f, used to obtain the friction force from $F_f = A\tau_f$, was adjusted to obtain the best agreement with the measured data, and the used value $\tau_f = 8$ MPa is similar to $\tau_f = 13$ MPa in the dry state and $\tau_f = 5$ MPa in the wet state, reported in ref. 17 (see also refs. 16 and 20). We observe that the frictional shear stress τ_f is usually independent of the asperity contact pressure $p^* = pA_0/A$ as long as p^* is less than a few megapascals. As an example, which is of interest for robotic or surgical grippers, for silicone rubber (polydimethylsiloxane) sliding (in complete contact) on a smooth glass surface at the sliding speed $v \approx 1$ mm/s, experiments have shown that $\tau_f \approx 0.1$ MPa (21). At the same sliding speed, for other types of rubber (22, 23) $\tau_f \approx 1 - 10$ MPa. This is also similar to what is observed for

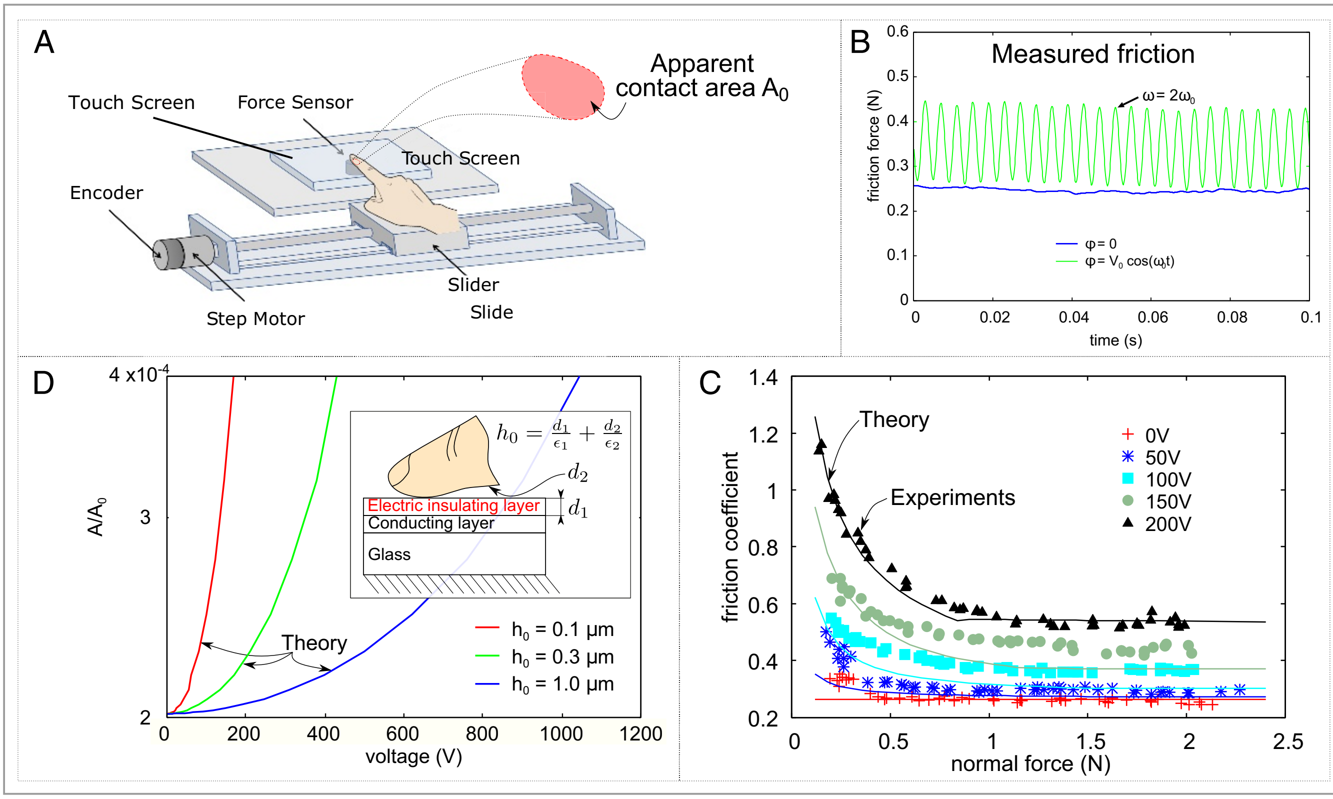

Fig. 3. Experimental and theoretical results. (*A*) Schematic of the experimental setup for measuring the force responses of the index finger in the normal and tangential directions, when subjected to a relative sliding motion with respect to the touchscreen. (*B*) Measured friction force F_f as a function of time. The green colored response was obtained by applying an oscillating electric potential to the touchscreen $\phi = V_0 \cos(\omega_0 t)$ [where $V_0 = 200$ V and $f_0 = \omega_0/(2\pi) = 125$ Hz]. (*C*) The friction coefficient μ obtained from the theory (solid lines) and the experiments (markers) as a function of the applied normal force F_N. The amplitude of the voltage applied to the touchscreen is varied between 0 V (red) and 200 V (black), with an increment of 50 V, at 125 Hz. The relative sliding speed in the experiments was 50 mm/s. In the calculations, we used $E_{SC} = 40$ MPa, $d = 200$ μm, $E_{bulk} = 10$ kPa, and $h_0 = 0.2$ μm. (*D*) The normalized contact area A/A_0 as a function of the applied voltage V and the thickness of the effective insulating layer $h_0 = d_1/\epsilon_1 + d_2/\epsilon_2$. The applied pressure is $p_0 = 10$ kPa.

plastics (polymers below the glass transition temperature) (24) and also as expected from molecular dynamics calculations (25).

Note that the friction coefficient increases when the applied normal force decreases, as is typical when adhesion is important. Note also that a small increase in the friction coefficient is also observed when the applied voltage is turned off. This has been observed also in earlier studies (26) and must be due to some additional adhesion process—for example, due to the van der Waals interaction—or due to capillary bridges formed by water or from oil on the fingers (27).

Finally, Fig. 3*D* shows the influence of the thickness of the effective insulating layer h_0 on the normalized contact area A/A_0 as a function of the applied voltage V. Note that $h_0 = d_1/\epsilon_1 + d_2/\epsilon_2$, however its value is mainly determined by the thickness of the touchscreen insulating layer. In the figure, the Young's modulus of the SC is $E_{\rm SC} = 100$ MPa, and the applied pressure is $p_0 = 10$ kPa. The results suggest that the thickness of the touchscreen insulating layer has a large impact on the normalized contact area and thus on the magnitude of the electroadhesive friction.

Discussion

The Effect of Electrovibration Frequency on Electoadhesion Force. Let us discuss how the frequency, ω, of the oscillating electric potential influences the electroadhesion force. Yamamoto and Yamamoto (28) have shown that SC has a finite electric conductivity. Thus, if the frequency is very small, charges can drift through the SC and to its outer surface. The theory described above is still valid in this limiting case: If ω is very small, the dielectric function of the SC is very large, and in fact $\epsilon_2(\omega) \to \infty$ as $\omega \to 0$. It follows that as $\omega \to 0$, we have $d_2/\epsilon_2 \to 0$, as if the insulating SC layer would not exist at all. This results in a shorter separation between the positive and negative charge distributions, and in order for the applied voltage to stay constant, the electric field in the air gap must increase. Clearly, in this case, the electroadhesion force would be maximal. The upper solid line in Fig. 4 shows the calculated dependency of the contact area on the frequency $f = \omega/(2\pi)$ of the oscillating electric potential $\phi = V_0 \cos(\omega t)$. The ratio $A_{\rm on}/A_{\rm off}$ between the real contact area with electroadhesion to that without electroadhesion was obtained using Eq. **3** with the dielectric function $\epsilon_2(\omega)$ of the SC given by Eq. **4** with $\epsilon_{\rm SC}(\omega)$ and $\rho_{\rm SC}(\omega)$ from ref. 28. We have used the normal force $F_{\rm N} = 0.5$ N and $V_0 = 100$ V, $d_1 = 1$ μm, $d_2 = 200$ μm, and $\epsilon_1 = 8$. At low frequencies, the charge on the skin surface can drift out on the touchscreen. This effect depends on the surface and bulk electric conductivity of the touchscreen and on liquids (e.g., oil and sweat), which may occur in some fraction of the noncontact area. To take this into account, we also show calculated results in Fig. 4 where we assume the airgap is filled with a material with the resistivity ρ equal to 10^5, 10^6, and 10^7 Ω m.

If we assume that the friction force is proportional to the area of real contact, then the ratio $A_{\rm on}/A_{\rm off}$ equals the ratio $\mu_{\rm on}/\mu_{\rm off}$ between the friction coefficient with electroadhesion to that without electroadhesion. The diamond symbols in Fig. 4 are experimental data for the ratio $\mu_{\rm on}/\mu_{\rm off}$.

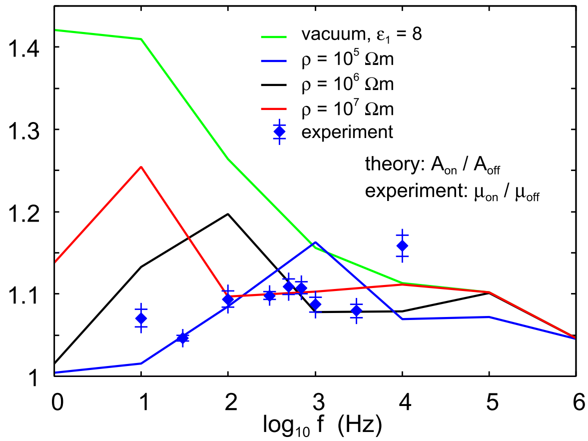

Fig. 4. (Solid lines) The calculated dependency of the contact area on the frequency $f = \omega/(2\pi)$ of the oscillating electric potential $\phi = V_0 \cos(\omega t)$. The $A_{\mathrm{on}}/A_{\mathrm{off}}$ is the ratio of the real contact area with electroadhesion to that without electroadhesion. The diamond symbols are the measured data for the ratio of friction coefficients with and without electroadhesion, $\mu_{\mathrm{on}}/\mu_{\mathrm{off}}$. See the first section in *Discussion* for details.

Note that similar experimental results were also obtained by Meyer et al. (9).

Tactile Perception of Elecrovibration. One interesting observation is that the electroadhesion between a finger and a touchscreen can be felt only indirectly as a change (increase) in the sliding friction force when an alternating voltage is applied to the touchscreen (also called electrovibration). That is, when a stationary finger is pushed against the touchscreen displaying electrostatic forces, the electrovibration cannot be perceived. The reason for this is the difference in the finger deformations between the conditions when the voltage is off and on and, accordingly, about the mechanoreceptors stimulated when the finger is stationary and moving.

For stationary contact, most of the electrovibration-induced deformations of the skin is localized to the SC. Hence, no mechanoreceptors experience stress to simulate the spiking response to convey information through nerve fibers to the brain. For sliding contact, instead, the additional friction force due to electroadhesion will result in a fluctuating shear deformation of the finger. Hence, the Pacinian corpuscles (FA II receptors), which are most sensitive to vibrations at 250 Hz (main frequency of the friction signal was 250 Hz; see Fig. 3*B*), will be deformed and emit neural signals (29). The discussions made by Vardar et al. (14) are in agreement with our arguments given above where they suggested that the Pacinian corpuscle is the primary mechanoreceptor responsible for the detection of the electrovibration stimuli. This is in line also with the study of Scheibert et al. (30), which emphasizes the role of fingerprints in stimulating the Pacinian receptors.

Limitations of the Study. In this study, we have assumed that the only attraction between the finger and the touchscreen is the electrostatic force due to the applied potential. In reality, there will always be other attractive interactions between two contacting solids; for example, the van der Waals interaction will operate between all solids, and capillary bridges can be very important for the human skin. Furthermore, we have neglected electrical breakdown across the narrow gap between the contacting solids (31). When a large electric potential is applied between narrowly separated surfaces, a very large electric field can prevail, in particular close to high and sharp asperities. If the local electric field becomes larger than some critical value, breakdown occurs. For gap separations that are typical in many applications (≈ 1 μm or less), the breakdown voltage is typically a few hundred volts. The relative importance of these additional effects will be evaluated in a future study.

The theory presented above focuses on the change in the contact area due to electroadhesion. It is true that the nominal (or apparent) contact area changes significantly (it decreases) with increasing tangential force, which we attribute to a large-strain nonlinear effect, but one expects from theory that the real contact area is nearly independent of the apparent contact area if the applied normal force is constant (and not too high). It is also known that the true contact area may decrease at the onset of sliding, but this is mainly the case when the surface roughness occurs on the harder surface and where the asperity contact regions renew during sliding. In any case, these "higher order" effects are not covered by our model.

Conclusion

We proposed a mean field theory based on multiscale contact mechanics to analyze the effect of electroadhesion on sliding friction. We performed experiments to measure how the friction between a finger and a touchscreen changes with the applied contact pressure and voltage under electroadhesion. We validated the proposed theory against the results of full-scale contact mechanics simulations and the experimental data. The proposed theory showed that electroadhesion produces an increase in real contact area, resulting in an increase in tangential frictional force. Also, we found that to further augment the friction force, and thus the human tactile sensing, a thinner insulating film could be used on the touchscreens. Finally, we explained the reason why haptic effects are not perceived when the finger is stationary but only when it is moving.

Materials and Methods

Electrostatic Attraction. In our model, we consider a contact between randomly rough soft solid and a rigid solid with a flat surface (Fig. 2 *A*, *1*), with an electric potential $\phi(t) = V_0 \ \cos\omega_0 t$ applied between the solids. This will give rise to an electric field in the air gap between the solids, resulting in an attractive force, which can be calculated from the *zz* component of the Maxwell stress tensor. Hence, the normal stress averaged over the surface roughness is (32)

$$\langle \sigma_{zz} \rangle = \frac{1}{4}\epsilon_0 V_0^2 \int_0^\infty du\, P(p,u)\,\frac{1+\cos(2\omega_0 t + 2\phi)}{|u + h_0(\omega_0)|^2}, \qquad [1]$$

where $P(p, u)$ is the probability distribution of interfacial separation u, which depends on the squeezing pressure p. We assume that the noncontact region, which is filled by air, is a vacuum because the dielectric constant of air ($\epsilon_{\mathrm{air}} \approx 1.00059$) is nearly the same as that of vacuum ($\epsilon = 1$, with absolute permettivity ϵ_0).

Assume that we squeeze the upper solid against the substrate with a normal force F_N. When an electric potential is applied between the solids, there will be an additional electric force acting on the solids. In the simplest approach, one includes the electric attraction $p_{\mathrm{a}} = \langle \sigma_{zz} \rangle$ as a contribution to the external load. Thus, we write the nominal effective squeezing pressure as

$$p = p_0 + p_{\mathrm{a}}, \qquad [2]$$

where $p_0 = F_N/A_0$ is the applied pressure. Intuitively, one expects this approach to be accurate when the interaction force between the surfaces is long-range. For example, a similar approach has been successfully used for investigating the attraction resulting from capillary bridges (27) (see also ref. 19).

To calculate $p_{\mathrm{a}} = \langle \sigma_{zz} \rangle$, we need to know the probability distribution $P(p, u)$. For randomly rough surfaces, the function $P(p, u)$ has been calculated using the theory of ref. 33. Using Eqs. **1** and **2**, the time (and space) averaged pressure becomes, after manipulation

$$V_0^2 = \frac{4(p - p_0)/\epsilon_0}{\int_0^\infty du\, P(p,u)|u + h_0|^{-2}}, \qquad [3]$$

from which one easily calculates V_0 as a function of p.

The dielectric function of the SC, which enters in Eq. **3** via $h_0 = d_1/\epsilon_1 + d_2/\epsilon_2$, can be written as

$$\epsilon_2(\omega) = \epsilon_{SC} + \frac{i}{\omega \epsilon_0 \rho_{SC}}, \quad [4]$$

where ϵ_{SC} and ρ_{SC} are both real quantities depending on the frequency ω. They have been measured for the human SC in a large frequency range by Yamamoto and Yamamoto (28).

Experiments. The main components of our skin tribometer include a high-torque step motor (moving a slide on a power screw) and a force sensor attached to the base of the touchscreen (SCT-3250, 3M), as shown in Fig. 3 *A*, *1*. The step motor (MDrive23Plus, Intelligent Motion Systems, Inc.) was programed to translate the slider with an alternative horizontal motion at the desired sliding velocity. The experimenter's hand was placed on the slider such that the phalanges of index finger were aligned to make an angle of approximately 30° with the touchscreen, and the tip of the index finger was always in contact with the touchscreen during the sliding. A sinusoidal voltage signal with amplitudes in the range of 50 V to 200 V at 125 Hz was applied to the touchscreen. As the experimenter's finger was moving on the touchscreen, the force response was measured using a force transducer (Nano 17, ATI Industrial Automation, Inc.). The normal and tangential forces were acquired by a 16-bit analog data acquisition card (NI PCI-6034 E, National Instruments, Inc.) with a sampling rate of 10 kHz.

All of the tests were performed for a stroke length of 40 mm at a sliding speed of 50 mm$/s$, which was selected based on the preliminary experiments so that full slip interface behavior was observed. For each applied voltage, the experimenter aimed to increase his normal force from 0.1 N to 0.9 N with an increment of 0.2 N after every other four strokes. To keep the normal force constant, the experimenter visually tracked his force response from a large screen oscilloscope and trained himself in advance of the experiments. However, it is important to emphasize that keeping the force at a constant value was not easy even for a trained experimenter and some deviations occurred.

ACKNOWLEDGMENTS. The authors are grateful to Dr. Ozgur Birer from Koc University for the FESEM micrographs. M.A. and M.S. acknowledge Forschungszentrum Jülich for the support and the kind hospitality received during their visit to the Peter Grünberg Institute-1, where most of their contribution to this work was performed. This work was performed within a Reinhart–Koselleck project funded by the Deutsche Forschungsgemeinschaft (DFG). B.N.J.P. thanks DFG for the project support under the reference German Research Foundation DFG-Grant MU 1225/36-1. M.S. acknowledges European Cooperation in Science and Technology Action CA15216 for Grant STSM-CA15216-40485. C.B. acknowledges the financial support provided by the Scientific and Technological Research Council of Turkey under Contract 117E954.

1. Wiertlewski M, Friesen RF, Colgate JE (2016) Partial squeeze film levitation modulates fingertip friction. *Proc Natl Acad Sci USA* 113:9210–9215.
2. Johnsen A, Rahbek K (1923) A physical phenomenon and its applications to telegraphy, telephony, etc. *J Inst Electr Eng* 61:713–725.
3. Mallinckrodt E, Hughes A, Sleator W, Jr (1953) Perception by the skin of electrically induced vibrations. *Science* 118:277–278.
4. Nakamura T, Yamamoto A (2017) Modeling and control of electroadhesion force in dc voltage. *ROBOMECH J* 4:18–28.
5. Shintake J, Rosset S, Schubert B, Floreano D, Shea H (2016) Versatile soft grippers with intrinsic electroadhesion based on multifunctional polymer actuators. *Adv Mater* 28:231–238.
6. Monkman G (2003) Electroadhesive microgrippers. *Ind Robot: Int J* 30:326–330.
7. Strong RM, Troxel DE (1970) An electrotactile display. *IEEE Trans Man-Machine Syst* 11:72–79.
8. Shultz CD, Peshkin MA, Colgate JE (2015) Surface haptics via electroadhesion: Expanding electrovibration with johnsen and rahbek. *World Haptics Conference (WHC), 2015 IEEE* (IEEE, Piscataway, NJ), pp 57–62.
9. Meyer DJ, Peshkin MA, Colgate JE (2013) Fingertip friction modulation due to electrostatic attraction. *World Haptics Conference (WHC), 2013* (IEEE, Piscataway, NJ), pp 43–48.
10. Xu C, Israr A, Poupyrev I, Bau O, Harrison C (2011) Tactile display for the visually impaired using teslatouch. *CHI'11 Extended Abstracts on Human Factors in Computing Systems* (ACM, New York), pp 317–322.
11. Tang H, Beebe DJ (1998) A microfabricated electrostatic haptic display for persons with visual impairments. *IEEE Trans Rehabil Eng* 6:241–248.
12. Kim SC, Israr A, Poupyrev I (2013) Tactile rendering of 3D features on touch surfaces. *Proceedings of the 26th Annual ACM Symposium on User Interface Software and Technology* (ACM, New York), pp 531–538.
13. Wijekoon D, Cecchinato ME, Hoggan E, Linjama J (2012) Electrostatic modulated friction as tactile feedback: Intensity perception. *International Conference on Human Haptic Sensing and Touch Enabled Computer Applications* (Springer, Heidelberg), pp 613–624.
14. Vardar Y, Güçlü B, Basdogan C (2017) Effect of waveform on tactile perception by electrovibration displayed on touch screens. *IEEE Trans Haptics* 10:488–499.
15. Grimnes S (1983) Electrovibration, cutaneous sensation of microampere current. *Acta Physiol* 118:19–25.
16. Persson BNJ, Kovalev A, Gorb SN (2013) Contact mechanics and friction on dry and wet human skin. *Tribology Lett* 50:17–30.
17. Kovalev AE, Dening K, Persson BNJ, Gorb SN (2014) Surface topography and contact mechanics of dry and wet human skin. *Beilstein J Nanotechnology* 5:1341–1348.
18. Dzidek B, Bochereau S, Johnson SA, Hayward V, Adams MJ (2017) Why pens have rubbery grips. *Proc Natl Acad Sci USA* 114:10864–10869.
19. Persson BNJ, Scaraggi M (2014) Theory of adhesion: Role of surface roughness. *J Chem Phys* 141:124701.
20. Adams MJ, Briscoe BJ, Johnson SA (2007) Friction and lubrication of human skin. *Tribology Lett* 26:239–253.
21. Chateauminois A, Fretigny C (2008) Local friction at a sliding interface between an elastomer and a rigid spherical probe. *Eur Phys J E* 27:221–227.
22. Rowe KG, Bennett AI, Krick BA, Sawyer WG (2013) In situ thermal measurements of sliding contacts. *Tribology Int* 62:208–214.
23. Lorenz B, Oh Y, Nam SK, Jeon SH, Persson BNJ (2015) Rubber friction on road surfaces: Experiment and theory for low sliding speeds. *J Chem Phys* 142:194701.
24. Whitten PG, Brown HR (2007) Polymer entanglement density and its influence on interfacial friction. *Phys Rev E* 76:026101.
25. Sivebæk IM, Samoilov VN, Persson BNJ (2008) Frictional properties of confined polymers. *Eur Phys J E* 27:37–46.
26. Derler S, Gerhardt LC, Lenz A, Bertaux E, Hadad M (2009) Friction of human skin against smooth and rough glass as a function of the contact pressure. *Tribology Int* 42:1565–1574.
27. Persson BNJ (2008) Capillary adhesion between elastic solids with randomly rough surfaces. *J Phys Condens Matter* 20:315007.
28. Yamamoto T, Yamamoto Y (1976) Dielectric constant and resistivity of epidermal stratum corneum. *Med Biol Eng* 14:494–500.
29. Saal HP, Delhaye BP, Rayhaun BC, Bensmaia SJ (2017) Simulating tactile signals from the whole hand with millisecond precision. *Proc Natl Acad Sci USA* 114:E5693–E5702.
30. Scheibert J, Leurent S, Prevost A, Debrégeas G (2009) The role of fingerprints in the coding of tactile information probed with a biomimetic sensor. *Science* 323:1503–1506.
31. Strong FW, Skinner JL, Dentinger PM, Tien NC (2006) Electrical breakdown across micron scale gaps in MEMS structures. *Reliability, Packaging, Testing, and Characterization of MEMS/MOEMS V*, eds Tanner DM, Ramesham R (SPIE, Bellingham, WA), Vol 6111, pp 611103-1–611103-9.
32. Persson BNJ (2018) The dependency of adhesion and friction on electrostatic attraction. *J Chem Phys* 148:144701.
33. Almqvist A, Campañá C, Prodanov N, Persson B (2011) Interfacial separation between elastic solids with randomly rough surfaces: Comparison between theory and numerical techniques. *J Mech Phys Sol* 59:2355–2369.